

We are IntechOpen, the world's leading publisher of Open Access books Built by scientists, for scientists

6,900

Open access books available

185,000

International authors and editors

200M

Downloads

Our authors are among the

154

Countries delivered to

TOP 1%

most cited scientists

12.2%

Contributors from top 500 universities



WEB OF SCIENCE™

Selection of our books indexed in the Book Citation Index
in Web of Science™ Core Collection (BKCI)

Interested in publishing with us?
Contact book.department@intechopen.com

Numbers displayed above are based on latest data collected.
For more information visit www.intechopen.com



Applications of Thermo-TDR Sensors for Soil Physical Measurements

Yili Lu, Wei Peng, Tusheng Ren and Robert Horton

Abstract

Advanced sensors provide new opportunities to improve the understanding of soil properties and processes. One such sensor is the thermo-TDR sensor, which combines the functions of heat pulse probes and time domain reflectometry probes. Recent advancements in fine-scale measurements of soil thermal, hydraulic, and electrical properties with the thermo-TDR sensor enable measuring soil state variables (temperature, water content, and ice content), thermal and electrical properties (thermal diffusivity, heat capacity, thermal conductivity, and bulk electrical conductivity), structural parameters (bulk density and air-filled porosity) and fluxes (heat, water, and vapor) simultaneously. This chapter describes the theory, methodology, and potential applications of the thermo-TDR technique.

Keywords: thermo-TDR sensor, heat pulse, time domain reflectometry, soil thermal properties, soil physical measurements

1. Introduction

Dynamic, in situ measurements of soil temperature (T), water content (θ), thermal and electrical properties are necessary to quantitatively evaluate coupled heat, water and solute transfer in soil. Ren et al. first introduced a thermo-time domain reflectometry (thermo-TDR) technique to measure T , θ , thermal properties, and bulk electrical conductivity (σ) [1]. Later, the thermo-TDR technique was advanced to determine soil bulk density (ρ_b), porosity (n), air-filled porosity (n_a), and water saturation from the above-mentioned properties [2]. Recent laboratory and field studies showed that the thermo-TDR technique could determine soil ice content during freezing and thawing, monitor coupled heat and water transfer processes, and describe soil structure changes and salt effect on soil [3–8]. Advantages of the thermo-TDR technique, e.g., minimal soil disturbance, ease in automation and multiplexing, providing point-scale data of soil thermal, electrical, and hydraulic variables and properties simultaneously, make it a state-of-the-art method for in-situ investigations of coupled soil processes.

In this chapter, the theories, methodologies and applications of the thermo-TDR technique are presented.

2. Theory and methodology of the thermo-TDR technique

2.1 Basic principles

The heat pulse technique can measure soil volumetric heat capacity (C), thermal conductivity (λ) and thermal diffusivity (κ) by analyzing the propagation of a heat pulse at a known distance from a line heat source [2, 9]. The TDR method determines the dielectric and electrical conductivity properties by sending an electromagnetic pulse along a metal TDR waveguide embedded in soil [10]. The pulse travel time is related to soil dielectric constant (K_a), and the attenuation of pulse amplitude is affected by soil σ [11]. The TDR sensor is widely used to measure soil θ from K_a using the equation from [10]. Noborio et al. and Ren et al. noticed the similarities in sensor materials and configurations between the heat pulse and TDR sensors, and integrated the two systems into a single unit, which was named the thermo-TDR sensor [1, 12]. The unified sensor combines the functions of the heat pulse sensor and TDR sensor, which allows thermal and electromagnetic pulses to be applied concurrently into the soil, and soil temperature, water content, thermal properties, and electrical conductivity are then determined simultaneously [1, 13].

2.2 Theories and calculations

2.2.1 Determination of soil thermal properties using the ILS theories

Thermo-TDR technique estimates soil thermal properties from the temperature change-by-time data at the sensing probes (heat pulse signals) based on line-source heat transfer models. The most widely known model is based on the infinite line source (ILS) theory considering an instantaneous or pulsed heating scheme, which assumes the heating probe as a line heat source with zero diameter and infinite length [9, 14–16]. For an isothermal and homogeneous soil with a uniform initial temperature distribution, the solution of the Fourier radial equation for heat conduction of a short-duration heat-pulse away from an infinite line source was developed by [17] further analyzed by [15, 16]. The temperature distributions in a cylindrical system are as follows:

$$T(r, t) = \begin{cases} T_1(r, t); & 0 < t \leq t_0 \\ T_2(r, t); & t > t_0 \end{cases} \quad (1)$$

where.

$$T_1(r, t) = -\frac{q}{4\pi\kappa C} \text{Ei}\left(\frac{-r^2}{4\kappa t}\right) \quad (2)$$

$$T_2(r, t) = \frac{q}{4\pi\kappa C} \left[\text{Ei}\left(\frac{-r^2}{4\kappa(t - t_0)}\right) - \text{Ei}\left(\frac{-r^2}{4\kappa t}\right) \right] \quad (3)$$

in which T is the temperature ($^{\circ}\text{C}$) at a radial distance r (m) away from the line heat source and at time t (s). t_0 is the heat pulse duration (s), $-\text{Ei}(-x)$ is the exponential integral, κ is soil thermal diffusivity ($\text{m}^2 \text{s}^{-1}$) and C is volumetric heat capacity ($\text{MJ m}^{-3} \text{K}^{-1}$). Soil thermal conductivity (λ , $\text{W m}^{-1} \text{K}^{-1}$) is calculated as the product of κ and C . The optimized κ and C values are derived by fitting Eq. (3) to the measured heat pulse signals. The variable q represents the quantity of heat liberated per unit length per unit time (J m^{-1}), which is calculated from the current (I , Amps) applied to the heater wire for a time of t_0 ,

$$q = I^2 R t_0 \tag{4}$$

where R is the resistance per unit length of the heating wire ($\Omega \text{ m}^{-1}$). The ILS model is widely used for heat pulse determined soil thermal properties, because of its simple form and computational efficiency.

2.2.2 Determination of soil thermal properties using the CPC solution

Ignoring the finite heat pulse probe properties (finite radius and finite heat capacity) can be a significant source of error when estimating soil thermal properties with the ILS theory, especially when there is a large contrast between the physical properties of probes and soil [18, 19]. Peng et al. [8] showed that finite probe effects on temperature rise with time curves were most significant in dry soils, and faded with increasing θ ; the ILS theory can cause about 6% relative error in dry soil thermal property estimates [20]. Knight et al. proposed a semi-analytical solution of the cylindrical perfect conductors (CPC) theory, accounting for the finite probe radius and finite probe heat capacity [18]. The CPC theory was successfully applied in various studies [19, 21, 22]. This is especially true for the large sensor designs, in which the CPC theory reduces the error due to the finite probe effects. The theories and applications of CPC theory can be found in [20].

Figure 1 shows typical heat pulse signals (temperature change-by-time data) in two sensing probes of a thermo-TDR measurement on a loamy sand soil with water content of $0.15 \text{ m}^3 \text{ m}^{-3}$. Generally, soil temperature starts to increase when the heat pulse is initiated and then decreases with time after the heat pulse ceases. The heating rate q equals 45.43 W m^{-1} (with a R of $888 \Omega \text{ m}^{-1}$, and a t_0 of 25 s). The CPC solution is applied to fit the measured data with the built-in nonlinear curve fitting functions (*nlinfit*) in MATLAB software (The Math Works Inc., Natick, MA). The estimated C and κ values are $1.59 \text{ MJ m}^{-3} \text{ K}^{-1}$ and $7.48 \times 10^{-7} \text{ m}^2 \text{ s}^{-1}$, respectively. Multiplying C and κ gives a λ value of $1.20 \text{ W m}^{-1} \text{ K}^{-1}$.

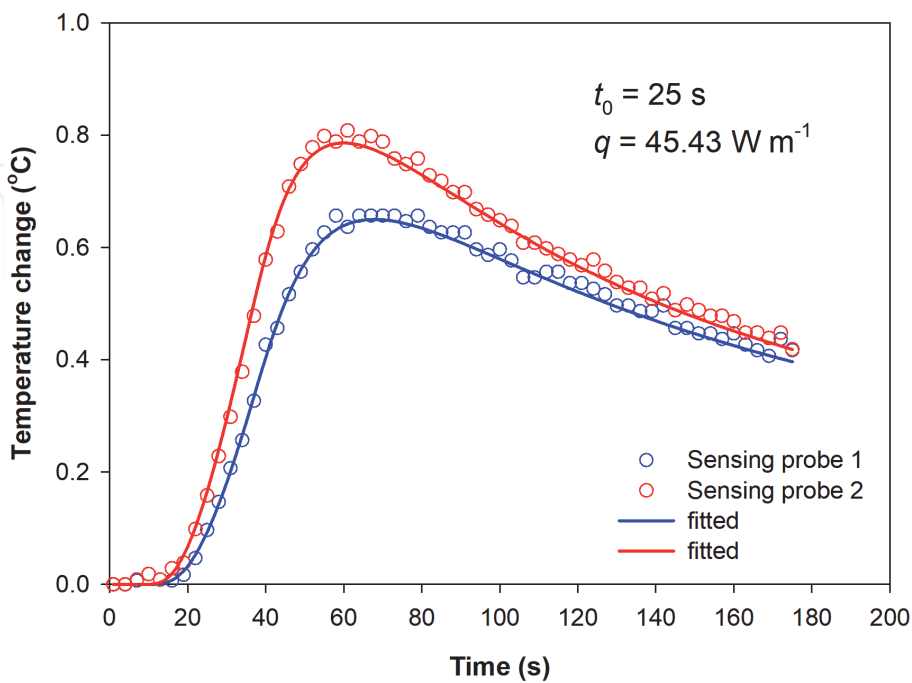


Figure 1. The temperature change-by-time data (circles) measured by two sensing probes with the large thermo-TDR sensor on a loamy sand soil. The lines represent the nonlinear curve fitting results for the CPC solution to the measured data. The heating duration (t_0) and the heating power (q) are listed.

2.2.3 Determination of soil water content and electrical conductivity

Soil θ and σ measurements are determined from the TDR waveforms obtained with the reflectometer device. **Figure 2** presents a typical TDR waveform generated with the TDR200 device (Campbell Scientific Inc., Logan, UT). The TDR technique determines K_a from the propagation time of an electromagnetic wave through a TDR wave guide. When an electromagnetic wave along the coaxial cable reaches the probe embedded in the soil, part of the signal is reflected back to the cable tester due to impedance change, which is shown as the first reflection point (L_1) on the waveform. The remaining signal travels continuously through the wave guide, and the second reflection point (L_2) is generated when the signal reaches the end of the probe due to impedance mismatch (**Figure 2**). Thus, K_a is calculated from [23],

$$K_a = \left(\frac{L_2 - L_1}{L_a} \right)^2 \quad (5)$$

where L_a is the apparent probe length (m), which needs to be calibrated before the thermo-TDR measurement.

Typically, L_1 and L_2 are determined with the tangent line method. For the short-probe thermo-TDR sensors, the tangent line-second-order bounded mean oscillation model (TL-BMO) method can be used to determine the reflections positions even when multi-reflections occur in short probes [24–26]. Both tangent line and TL-BMO methods are built-in algorithms in the TDR200 reflectometer device for calculating soil K_a . To estimate soil θ , the Topp et al. equation or a specific calibration of the K_a - θ relation can be used [10].

The magnitude of soil σ depends on the transmission line impedance R_{total} (Ω), which can be calculated from the amplitude of the TDR signal at very long times [27, 28],

$$R_{\text{total}} = Z_c \frac{1 + \rho_{\infty}}{1 - \rho_{\infty}} \quad (6)$$

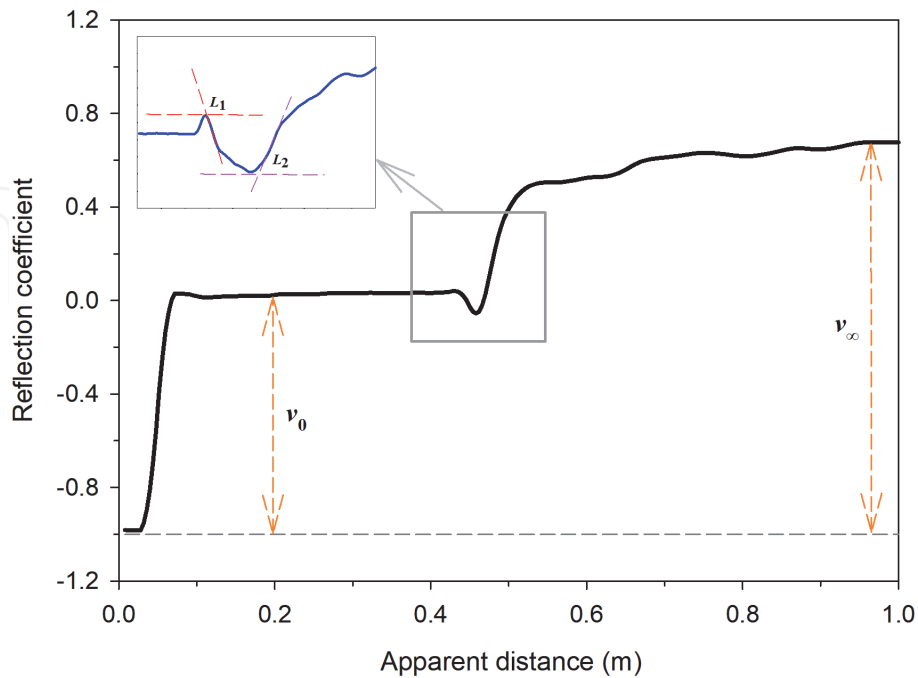


Figure 2.

A TDR waveform from the thermo-TDR sensor immersed in distilled water. v_0 is the amplitude of the incident voltage waveform generated by cable tester, and v_{∞} is final voltage amplitude in the transmission line after all multiple reflections have ceased. Part of the waveform framed in gray is used for water content calculation. L_1 and L_2 are the first and second reflection points on a TDR waveform (from [8]).

where Z_c is the characteristic impedance of the cable (75Ω); ρ_∞ is the voltage reflection coefficient at long times where multiple reflections have ceased with the TDR waveform reaching a stable level, which is defined as,

$$\rho_\infty = \frac{v_\infty - v_0}{v_0} \quad (7)$$

where v_0 is the amplitude of the incident voltage waveform generated by the cable tester, and v_∞ is final voltage amplitude in the transmission line after all multiple reflections have ceased (**Figure 2**).

Following Heimovaara et al. σ can be obtained with the following equation [29],

$$\sigma = \frac{K_p}{R_{\text{total}} - R_c} f_T \quad (8)$$

where K_p is the cell constant of probe ($\sim 8.77 \text{ m}^{-1}$) determined by using the method in [29] with different KCl solutions; R_c is the combined series resistance of the cable, connectors, and cable tester, and f_T is the temperature factor,

$$f_T = \frac{1}{1 + \delta(T - 25)} \quad (9)$$

in which δ is the temperature coefficient of the soil sample ($0.0191^\circ\text{C}^{-1}$, [29]), and T ($^\circ\text{C}$) is the temperature of soil sample at the measurement time. Previous studies showed that R_c in Eq. (8) was only a small fraction of the R_{total} , which could be neglected without serious errors [30]. Wang et al. incorporated a piece-wise model for electrical conductivity calculations into the TL-BMO model for an accurate determination of σ , θ and K_a simultaneously [31]. The corresponding computer program is available at <https://github.com/cauwzj>.

2.3 Sensor configuration and construction

The design of the thermo-TDR sensor must meet several criteria to achieve the requirements of line-source heat-pulse theory to measure soil thermal properties and TDR principles to derive soil water content and electrical conductivity [1, 22]. The key parameters are probe diameter (d), probe length (L) and probe-to-probe spacing (r). For the heat pulse measurement, $L/d > 25$, $L/2r > 2.2$, and $d/2r < 0.13$ should be considered to minimize the effects of axial heat flow and finite probe properties on soil thermal property measurements [15, 16, 32]. A r/d value less than 10 is necessary for reliable TDR data [33].

Various configurations have been proposed for the thermo-TDR sensor. The original sensor design consisted of three parallel probes with 40-mm length, 1.3-mm diameter, and 6-mm probe-to-probe spacing [1] (**Figure 3**). The middle probe acted as a heater that introduced a heat pulse into soil, while the two outer needles acted as the sensing probes that measured the soil temperature at a known distance (e.g., $\sim 6 \text{ mm}$) from the heating probe.

Newer versions of thermo-TDR sensor designs, with various probe sizes and configurations (i.e., L , r , d) have been developed to enhance the strength and robustness of the sensor. Liu et al. presented a sensor design to obtain accurate soil thermal properties and ρ_b values under field conditions, by using large-size probes (45-mm length, 2-mm in diameter, and 8-mm probe-to-probe spacing) and adding pointed tips at the probe ends [34]. A similar design, with pointed tips, 40.5-mm length, 2-mm diameter, and 6-mm probe-to-probe spacing, was used by Yu et al. in

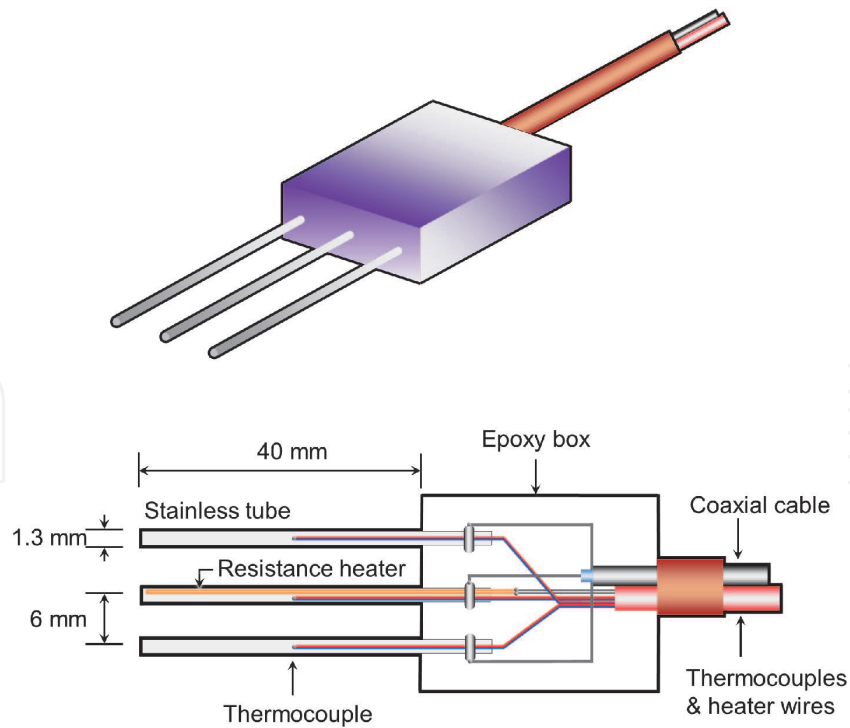


Figure 3. Schematic view of the thermo-TDR sensor configuration in [1]. (Figure originally published in [2]).

geothermal applications [35]. Wen et al. introduced a thermo-TDR sensor with relatively thin (1.27-mm) and long (60 mm) probes, but was capable of in situ corrections of r changes due to probe deflection [36]. A sensor with curved heaters was tested, but it introduced potential errors due to soil compaction caused by the relatively large heaters [37].

The small sensing volume of the Ren et al. sensor design made it suitable for fine-scale measurements, but the short probes somewhat restricted the accuracy of TDR measurements [1, 38]. Recently Peng et al. introduced a large-size thermo-TDR with a probe length of 70 mm, and a probe-to-probe spacing of 10-mm, a diameter of 2.38 mm for the heater probe, and a diameter of 2 mm for the sensing probe (**Figure 4**) [22]. As a result, this sensing volume was three times larger than that of the Ren et al. [1] sensor, and greater accuracy was achieved with TDR θ measurement accuracy due to the reduction of the superimposed reflections. Peng et al. also integrated updated algorithms to determine soil thermal and dielectric properties in order to produce accurate θ , ρ_b and porosity values [22].

Thermo-TDR sensors are not readily commercially available. One may be able to make special order sensors from some companies, but in most cases the sensors are constructed in soil physics research laboratories. As shown in **Figure 3**, a thermo-TDR sensor usually consists of three probes that house the heating wire and temperature sensors (thermocouples or thermistors), an epoxy base that fixes the probes in place, extension wires for the heater and temperature sensors, and a coaxial cable for TDR measurement. The stainless-steel tubes that serve as housings for heating and sensing probes, can be custom made or produced from hypodermic needles with the specified diameter and length.

The heating probe is constructed by threading an enameled resistance heater wire (e.g., 38-gauge Nichrome 80 Alloy), through the heating needle two or four times for a total resistance of about $888 \Omega \text{ m}^{-1}$. The sensing probes are typically constructed by positioning a thermocouple or a thermistor enclosed at the midpoint

Materials	Specifications
Thermocouple	Type E, chromel-constantan, 40 AWG, OMEGA Engineering, CT
Thermocouple extension wire	Type E, chromel-constantan, 36 AWG, OMEGA Engineering, CT
Thermistor	Model 10K3MCD1, 0.46-mm diam., 10 k Ω at 25°C; Betatherm Corp., Shrewsbury, MA
Resistance wire	79- μ m diameter, 40 AWG, enameled, 205 Ω m ⁻¹ , Nichrome 80 Alloy, Pelican Wire Co., Naples, FL
Stainless-steel tube	Ren et al. : 1.27-mm o.d. and 0.84-mm i.d for both heating and sensing probes [1]. Peng et al. : 2.38-mm o.d., 0.71-mm wall thickness for heating probe, 2.00-mm o.d., 0.25-mm wall thickness for sensing probes [22].
Coaxial cable	75 Ω coaxial cable, RG 187 A/U, Newark Electronics
Epoxy inside probes	High thermal conductivity, Omegabond 101, Omega Engineering, Stamford, CT
Casting resin for sensor body	Water proof, Cr600 Casting Resin, Micro-Mark, Berkeley Heights, NJ

Table 1.
Materials used for making thermo-TDR sensors.

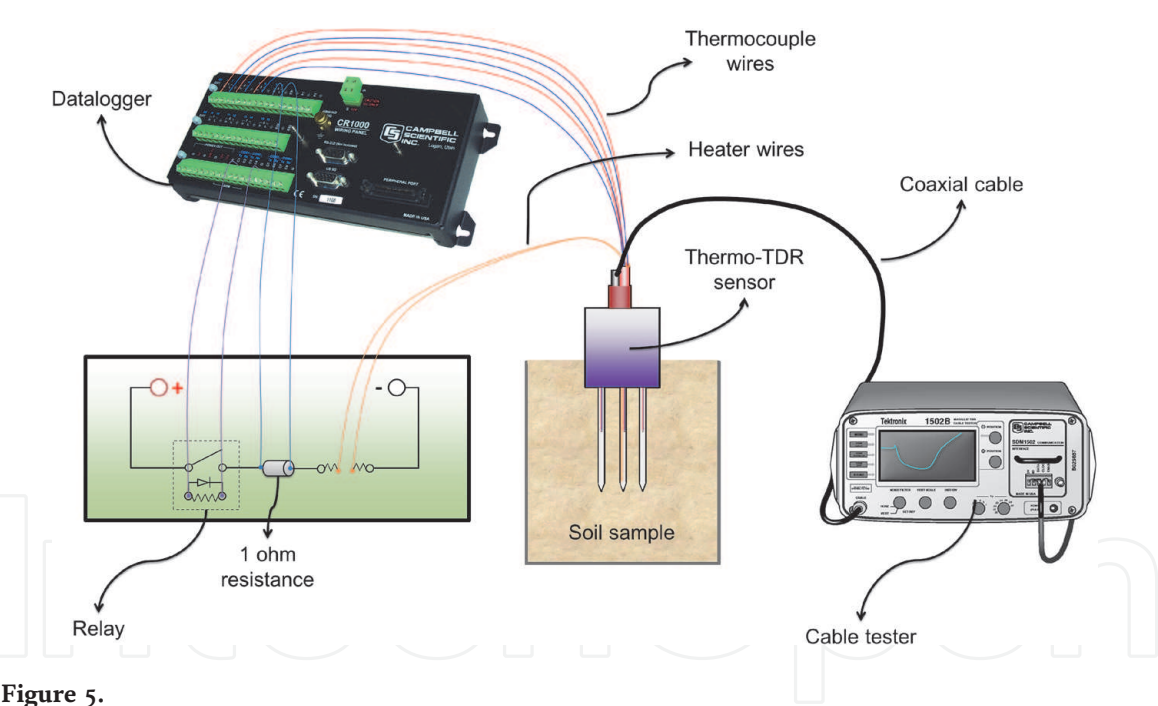


Figure 5.
Experiment setup for a typical thermo-TDR measurement.

activated by the datalogger. The resistance wire is heated for a controlled amount of time (typically 8–20 s for small sensors and 15–30 s for large sensors). During the heat pulse process, the current in the heater wire is determined automatically by measuring the voltage drop across a 1- Ω precision resistor which is in series with the heater wire.

Once the measurement is initiated, the current in the resistance wire and soil temperatures of the sensing probes are recorded at a 1-s interval for about 100–300 s with a datalogger (e.g., model CR1000x or CR3000, Campbell Scientific Inc., Logan, UT). The total measurement time can be set to be longer than 300 s, especially when the background soil temperature varies significantly with time under the field conditions. In this case, a linear temperature correction procedure is

needed for the soil thermal property calculations [39, 40]. The heating intensity should be carefully controlled to achieve a clear heat pulse signals at the sensing probe and to avoid potential heat induced moisture redistributions at the same time. Normally, the heat pulse duration is set to make sure that the temperature changes at the sensing probes typically fall in the range of 0.5–1.0°C.

The thermo-TDR sensor can be placed horizontally or vertically in a soil profile, depending on the application objectives. Special care is required to avoid needle deflection and to keep good soil-probe contact during installation. It is recommended to install the sensor under moist conditions when probe deflection is less likely to occur [2].

2.5 Sensor calibrations

Accurate information about parameters r , L and K_p are needed to determine soil thermal properties, water content, and electrical conductivity with the thermo-TDR technique. A 2% change in r value can induce 4% error in C estimates. The probe-to-probe spacing r is frequently calibrated in a medium with a known C value at room temperature, such as agar-stabilized water (at a concentration of 5 g L⁻¹) with a C value equal to that of water (4.18 MJ m⁻³ K⁻¹, [9]). The r value is calculated by nonlinear curve fitting to the measured heat pulse data based on ILS or CPC theory.

Wen et al. designed a probe-spacing-correction thermo-TDR sensor with 6-cm long sensing probe, each enclosed with three thermistors at different distances away from the sensor base [36]. This enabled the calculation of probe deflection angles to estimate actual in situ r values by using linear and nonlinear models proposed by [41, 42]. In field applications, Zhang et al. proposed an on-site calibration method that determined the in-situ r value by using the theoretical C values estimated from a one-time ρ_b and θ calibration using an intact soil core collected near the sensor location [43].

For K_a and θ measurements with the thermo-TDR sensor, the L_a of the sensor is calibrated by analyzing the TDR waveform obtained in distilled water at room temperature, which is calculated as,

$$L_a = \frac{L_2 - L_1}{V_p \sqrt{K_w}} \quad (10)$$

where K_w , apparent dielectric constant of water (80.1 at 20°C, Haynes and Lide, 2010). V_p is a user-selected propagation velocity, which is usually set as 0.99. L_1 can be determined by shorting the three needles in air with a razor blade at the needle base [44].

For TDR- σ measurements with the thermo-TDR sensor, K_p of the thermo-TDR sensor can be estimated following the procedures of [29]. The sensor is immersed in KCl solutions with a series of concentrations (e.g., 0.0001, 0.0005, 0.001, 0.005, 0.01, 0.02, 0.1, and 1.0 mol L⁻¹), and the TDR waveforms are collected. The voltage reflection coefficient at long times is determined from the TDR waveforms, from which R_{total} is calculated. Meanwhile, the solution σ is measured with a conductivity meter. The K_p value of the improved thermo-TDR sensor and R_c are then estimated by using regression analysis of σ vs. R_{total} [1, 8].

3. Applications of the thermo-TDR technique

3.1 Determination of soil thermal property and electrical conductivity curves

The thermo-TDR technique permits routine measurements of soil thermal properties, water content and electrical conductivity on repacked soil columns and

in situ field measurements. **Figure 6** presents the results of soil thermal properties on a repacked sand soil, showing typical trends of C , λ , and κ in relation to θ . Generally, C is linearly related to θ , while κ and λ vary nonlinearly with θ . Both κ and λ show rapid increases at $\theta < 0.10 \text{ m}^3 \text{ m}^{-3}$, and afterwards λ continuously increases while κ values decrease. These typical trends agree with published soil thermal property datasets, and earlier studies of C , λ , and κ models in relation to soil texture, water content, porosities [45–47].

Figure 7 shows measured apparent σ values for sand wetted by various salt solution concentrations to θ ranging from 0.08 to $0.25 \text{ m}^3 \text{ m}^{-3}$. It is clear that the increases in salt concentrations lead to significant increases in σ , and σ also increases with θ . Soluble salt ions in soil solution can enhance the electric conductivity of bulk soil. For salt affected soils, the Peng et al. [8] thermo-TDR sensor can measure σ values as large as 22.5 dS m^{-1} . Thus, important observations of solute, heat and water properties in soil are possible with thermo-TDR sensors.

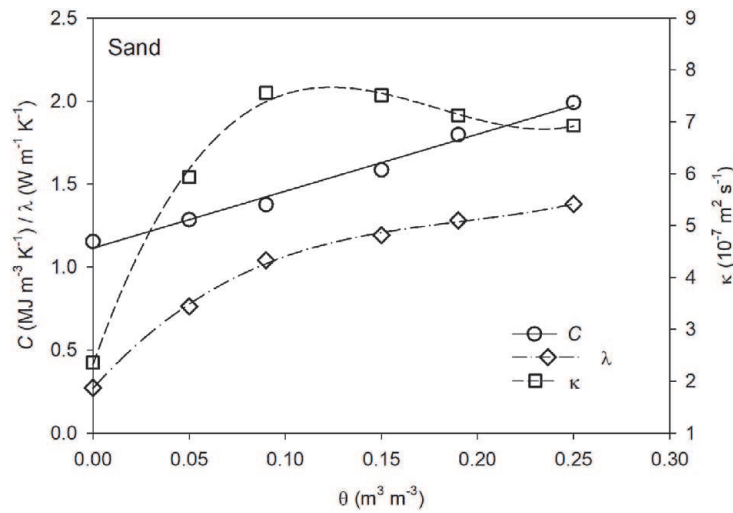


Figure 6. Thermo-TDR determined thermal properties of a sand at bulk density of 1.47 Mg m^{-3} as a function of water content.

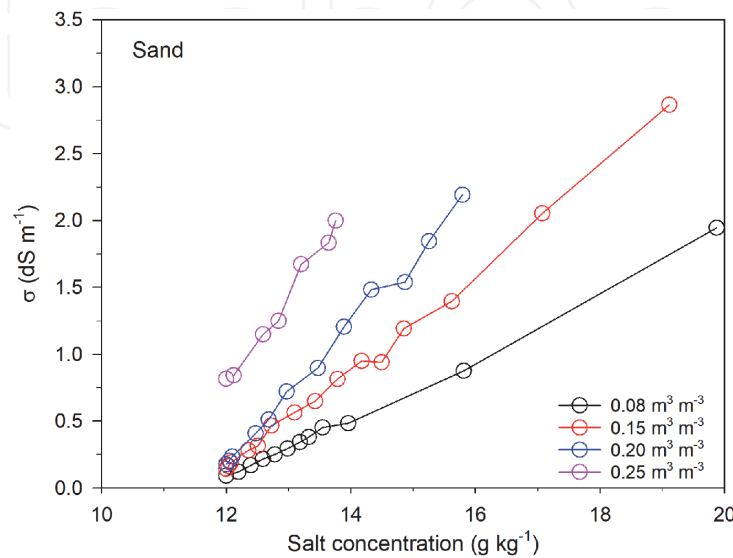


Figure 7. Thermo-TDR measured bulk electrical conductivity of a sand soil as a function of KCl salt concentrations used to wet the soil to four selected water contents.

3.2 Determination of soil bulk density, porosity and air-filled porosity

The thermo-TDR technique soil thermal property and water content data can be used to estimate soil structure changes [43, 48, 49]. The thermo-TDR technique can be applied to determine in situ ρ_b , n and n_a based on three quantitative relationships of ρ_b and θ with C , λ , e.g., de Vries, the Lu et al. and the Tian et al. models [45, 50, 51].

Thermo-TDR determinations of ρ_b depend on the de Vries C model (hereafter C -based thermo-TDR method) and the Lu et al. or Tian et al. λ model (hereafter λ -based thermo-TDR method) [45, 50, 51]. According to [45], soil C can be estimated as the weighted sum of volumetric heat capacities of soil solids, water and air. As the volumetric heat capacity of air is small compared to those for soil solids and water, soil C can be approximated as [9],

$$C = \rho_b c_s + \rho_w c_w \theta \quad (11)$$

From Eq. (11), ρ_b is derived as,

$$\rho_b = \frac{C - \rho_w c_w \theta}{c_s} \quad (12)$$

where c_s is the specific heat of soil solids ($\text{kJ kg}^{-1} \text{K}^{-1}$), ρ_w is the density of water (1.0 g cm^{-3}), and c_w is the specific heat of water ($4.18 \text{ kJ kg}^{-1} \text{K}^{-1}$) [9]. Once soil C and θ are determined from a thermo-TDR measurement, ρ_b can be calculated with Eq. (12). It was pointed out that the C -based thermo-TDR method for determining ρ_b was likely affected by changes in probe-to-probe spacing when inserting the sensor into soil [52, 53]. Liu et al. reduced such errors by increasing the rigidity of the sensor design, and obtained the continuous field ρ_b for the tilled soil layers which changed over time with wetting and drying cycles [34, 48].

Because λ measurements using the heat pulse technique are not influenced by needle deflection, Lu et al. proposed the λ -based thermo-TDR method to determine in situ ρ_b [54]. An empirical equation that related λ to ρ_b , θ , and soil texture was used [50],

$$\lambda = \lambda_{\text{dry}} + \exp(b - \theta^{-a}) \quad \theta > 0 \quad (13)$$

where a and b are shape factors that are estimated from ρ_b and fractions of sand and clay,

$$\begin{cases} a = 0.67f_{\text{cl}} + 0.24 \\ b = 1.97f_{\text{sa}} + 1.87\rho_b - 1.36f_{\text{sa}}\rho_b - 0.95 \end{cases} \quad (14)$$

where f_{sa} and f_{cl} are fractions of sand and clay, respectively, under the USDA soil textural classification system. The thermal conductivity of dry soils (λ_{dry}) relates linearly with n [46]. For mineral soils, setting soil particle density (ρ_s) as 2.65 g cm^{-3} , λ_{dry} is calculated from [46],

$$\lambda_{\text{dry}} = -0.56n + 0.51 = -0.56\left(1 - \frac{\rho_b}{\rho_s}\right) + 0.51 \quad (15)$$

An iterative approach is used to numerically solve for ρ_b because there is no explicit solution for ρ_b from Eqs. (13)–(15). The nonlinear equation solver (*fsolve*) in MATLAB (Mathworks, Inc., Natick, MA) can be applied using an initial ρ_b value of 1.0 g cm^{-3} .

The empirical Lu et al. λ model introduced uncertainty in ρ_b estimates, especially for coarse soils [50]. Thus, Tian et al. proposed a simplified version of the physically-based de Vries λ model to inversely estimate ρ_b , and they found that their λ model performed better than the C model and other empirical λ models [49]. When applying λ -based thermo-TDR methods on relatively dry soils, accurate θ inputs are required, because λ values of dry soils are insensitive to small θ changes. Therefore, Peng et al. used a combined approach to determine ρ_b : the C -based approach was used when θ was less than $0.10 \text{ m}^3 \text{ m}^{-3}$, and the λ -based approach was used at $\theta > 0.10 \text{ m}^3 \text{ m}^{-3}$ [22].

Both C - and λ -based thermo-TDR methods rely on TDR determined θ values as inputs. Lu et al. introduced a heat pulse based approach to determine ρ_b with only C and λ values [55]. This method relies on the de Vries C model and the Lu et al. λ model with known soil texture and c_s as a priori, and calculates ρ_b with an interactive procedure [45, 50]. The heat pulse based approach can be used when TDR θ is not readily available. Peng et al. [20] showed that on salt affected soils where the accuracy of TDR θ was greatly restricted, using the heat pulse based method provided more accurate determinations of θ and ρ_b values than the thermo-TDR based method [8].

It is commonly recognized that a tilled soil layer undergoes great structural changes due to agricultural management and rainfall effects. The in situ measurements of ρ_b in tilled soil layers using a thermo-TDR technique indicated that soil ρ_b increased following tillage because rainfalls caused soil particles to settle and consolidate [48, 49]. **Figure 8** shows that soil ρ_b increased and then leveled off, and the thermo-TDR method determined ρ_b values mostly matched the core sample values.

With the thermo-TDR determined θ and ρ_b , soil n can be calculated with known soil particle density ($\rho_s = 2.65 \text{ g cm}^{-3}$),

$$n = 1 - \frac{\rho_b}{\rho_s} \quad (16)$$

Thus, the n_a and degree of water saturation (S_w) values can be calculated,

$$n_a = n - \theta \quad (17)$$

$$S_w = \frac{\theta}{n} \quad (18)$$

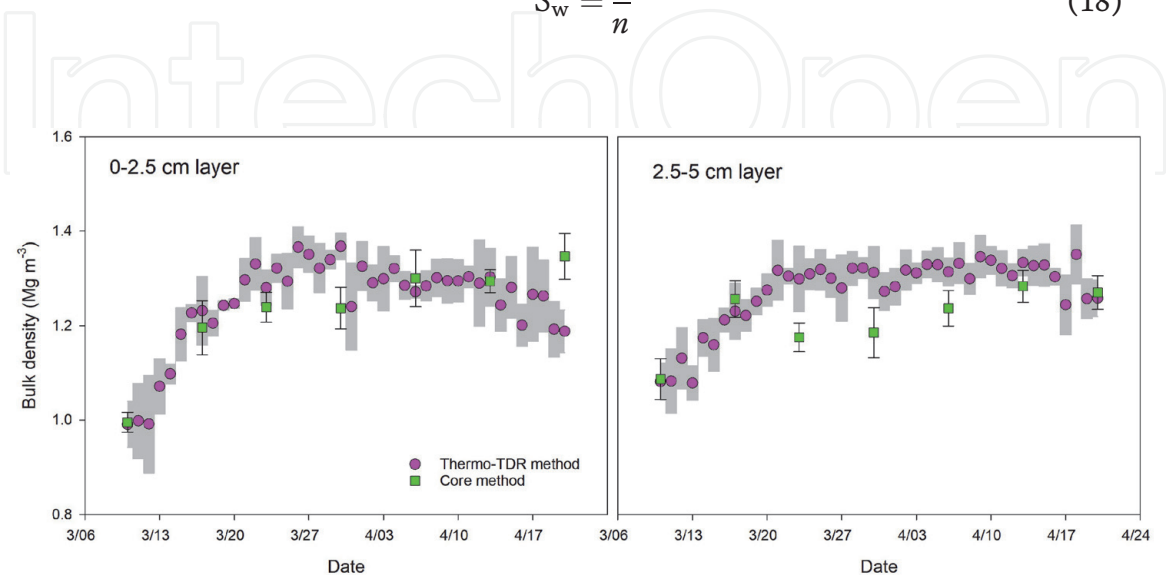


Figure 8. Dynamic thermo-TDR measured bulk density (ρ_b) values for two soil layers plotted along with independent ρ_b values from soil core measurements. Both error bars and gray areas represent standard errors of the measurements (figure originally published in [49]).

Fu et al. [56] showed that when applying the thermo-TDR technique in cropped soil, the influences of roots should be considered by using an extended mixing model based on Eq. (11),

$$C = f_s C_s + f_w C_w + f_{rw} C_w + f_r C_r \tag{19}$$

where f_s, f_w, f_{rw} and f_r are volume fractions of soil solids, soil water, root water and dry root, respectively; C_s and C_r are the volumetric heat capacity of soil solids and dry roots (assumed to be equal to the volumetric heat capacity of organic materials, $2.51 \text{ MJ m}^{-3} \text{ K}^{-1}$ at 20°C , [45]), respectively.

For a bulk soil sample with a volume of V , Eq. (19) can be rewritten as [57],

$$C = \frac{m_s}{V} c_s + \left(\frac{V_w}{V} + \frac{V_{rw}}{V} \right) C_w + \frac{V_r}{V} C_r \tag{20}$$

where V_w, V_{rw} and V_r are the volumes of soil water, root water and dry roots, respectively, and m_s is the dry mass of soil solids. By rearranging Eq. (27), the root zone ρ_b can be derived as,

$$\rho_b = \frac{m_s}{V - V_{rw} - V_r} = \frac{C - \theta_{\text{total}} C_w - \frac{V_r}{V} C_r}{c_s(1 - \theta_{\text{total}})} \tag{21}$$

where

$$\theta_{\text{total}} = \frac{V_w + V_{rw}}{V} \tag{22}$$

where θ_{total} is defined as the sum of volumetric θ values of root and soil. Fu et al. report that when the maize root density is greater than 0.037 g cm^{-3} , Eqs. (21, 22) should be used to estimate ρ_b from thermo-TDR measured C and θ [57]. The soil profile root density distribution is needed to estimate ρ_b in the root zone. **Figure 9** presents the results of thermo-TDR ρ_b estimates and the actual ρ_b in a maize root zone, and using the extended approach improves the accuracy of thermo-TDR ρ_b estimates by accounting for the influence of roots during the maize growing season. Thus, it is important to consider the influence of roots when applying the thermo-TDR technique in crop fields.

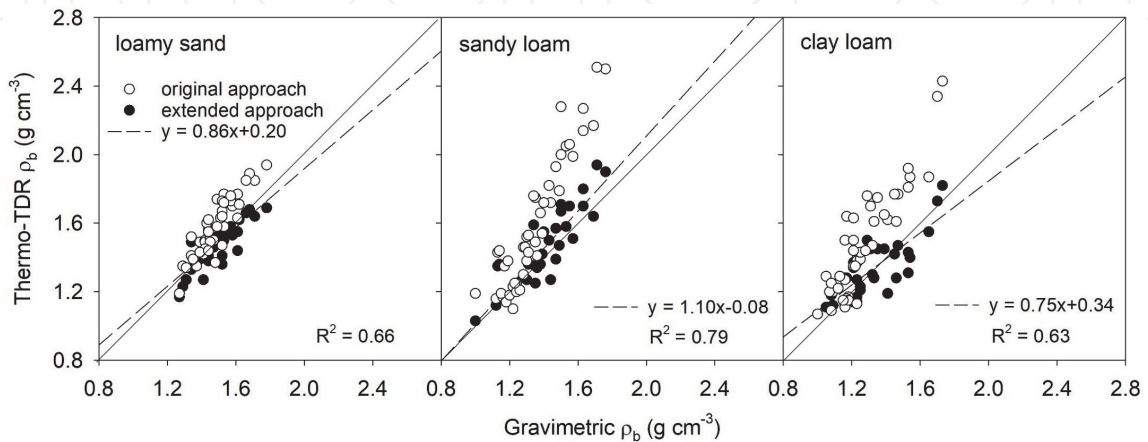


Figure 9. Comparison of thermo-TDR soil bulk density (ρ_b) estimates from the original approach (Eq. (12)) and the extended approach (Eq. (21)). (figure originally published in [57]).

3.3 Measuring soil ice contents during freezing and thawing

Although in-situ determination of soil ice content during freezing and thawing is challenging, a thermo-TDR technique has been developed to measure soil liquid water and ice contents in partially frozen soils. Tian et al. report that thermo-TDR determined heat capacity and liquid water content in partially frozen soil can be used to determine soil ice content [4]. According to [45], the volumetric heat capacity of a partially frozen soil can be expressed as,

$$C = f_s C_s + \theta_u C_u + f_a C_a + \theta_i C_i \quad (23)$$

where f_s , θ_u , f_a and θ_i are the volume fractions of soil solids, unfrozen water, air and ice, respectively. C_s ($2.35 \text{ MJ m}^{-3} \text{ K}^{-1}$), C_u ($4.18 \text{ MJ m}^{-3} \text{ K}^{-1}$), C_a ($0.0012 \text{ MJ m}^{-3} \text{ K}^{-1}$), and C_i ($1.73 \text{ MJ m}^{-3} \text{ K}^{-1}$) are volumetric heat capacities of soil solids, unfrozen water, air and ice, respectively [58]. C_a is very small compared to other soil constituents which can be neglected. The term f_s can be calculated from the ratio of ρ_b and ρ_s .

Tian et al. reported that the heating strength of heat pulse measurements should be carefully controlled for measurements in partially frozen soil to minimize ice melting during the process [4]. Their results indicated that the heat pulse method failed to provide accurate thermal properties at soil temperatures between -5 and 0°C because of temperature field disturbances from latent heat of fusion. The optimized heating application strategy was found to be a 60-s heat duration (450 J m^{-1}) or a 90-s heat duration ($450\text{--}900 \text{ J m}^{-1}$), and the C -based approach could only be applied at soil temperature $\leq -5^\circ\text{C}$. **Figure 10** shows the results of thermo-TDR determined ice contents on three soils with total water content (θ_t) of $0.15 \text{ m}^3 \text{ m}^{-3}$ during freezing and thawing periods in a soil column experiment. Soil ice began to form when the temperature was below 0°C because of the supercooling effect. A large portion of latent heat was released during ice formation, which led to unstable thermo-TDR θ_i values during this period. The measurement errors were within $\pm 0.05 \text{ m}^3 \text{ m}^{-3}$ when soil temperatures were below -5°C [4].

Tian et al. reported that the C -based approach was prone to errors resulting from probe deflections due to ice expansion during freezing [5]. The λ -based approach using the simplified de Vries model was used to determine the ice content with inputs of λ , ρ_b , and TDR- θ_u , and it was also reported to perform well at temperatures of -1 and -2°C , thus extending the measurement range near 0°C . It was noted that both C -based and λ -based approaches required accurate ρ_b information.

For soils experiencing seasonal or diurnal freezing and thawing cycles, Kojima et al. proposed an approach with TDR- θ determinations made before and after an imposed ice melting process caused by heating the soil surrounding the sensor [7]. The θ_i value was equivalent to the difference between the two TDR- θ values, which represented the liquid water content and total water content in the soil. Their method only relied on the two TDR- θ values but required long measurement intervals and a relatively large heat input to melt the ice.

3.4 Measuring heat, water, and water vapor fluxes in soil

The thermo-TDR method is a useful tool that can be used in laboratory and field experiments to study transient in-situ properties and processes related to coupled heat and water transfer in soil. Heitman et al. used thermo-TDR sensors in a closed soil cell with imposed transient boundary conditions to obtain non-uniform temperature, water and thermal property distributions [3]. Thermo-TDR sensors were

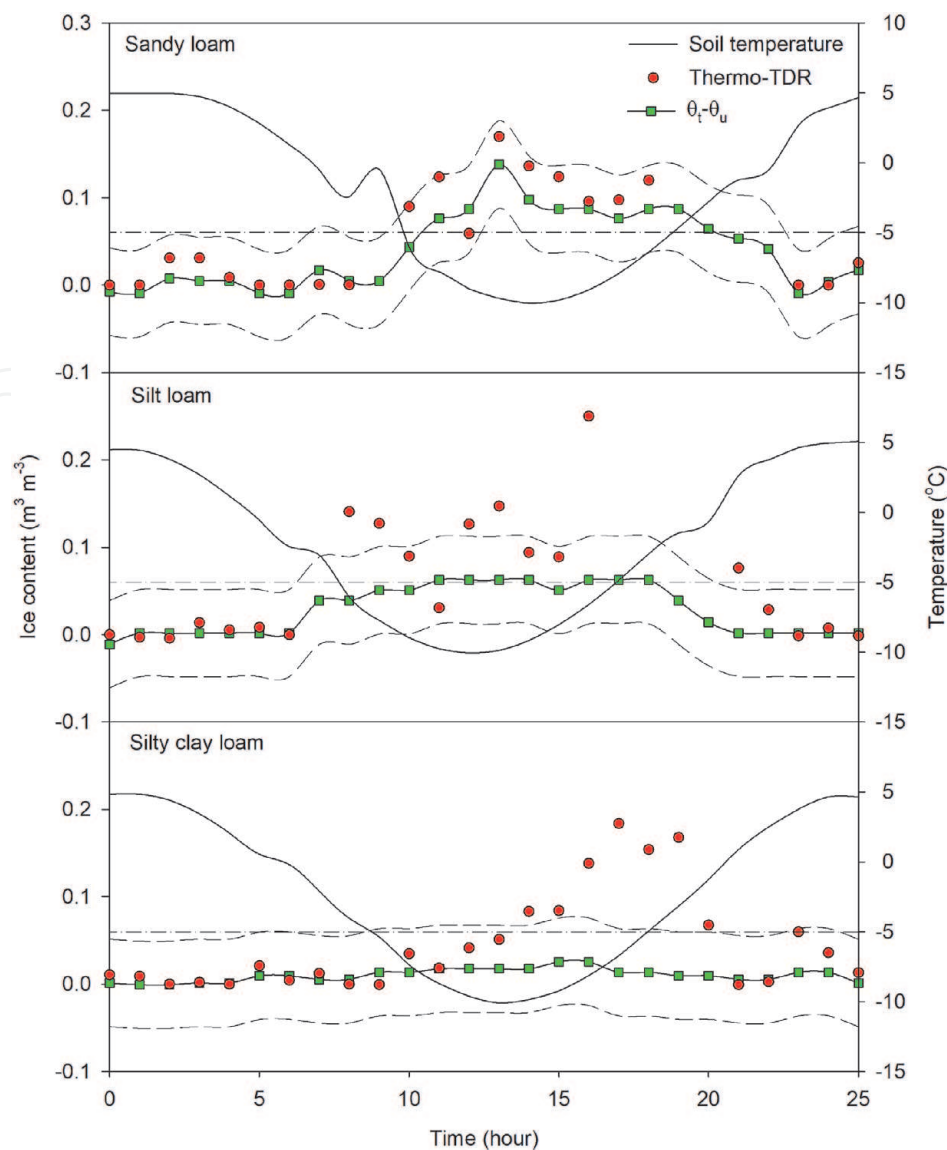


Figure 10. Soil temperature dynamics, thermo-TDR measured ice contents (from Eq. (30)), and TDR evaluated ice contents ($\theta_t - \theta_u$) during freezing and thawing for soil samples with a water content of $0.15 \text{ m}^3 \text{ m}^{-3}$ on sandy loam, silt loam and silty clay loam soils. Dashed lines indicate $\pm 0.05 \text{ m}^3 \text{ m}^{-3}$ error. (figure originally published in [4]).

used to obtain soil thermal conductivity during wetting and drying processes on quartz sands for geothermal applications [59–62].

Significant improvements in both sensor configurations and theories have been made in fine-scale measurements of coupled water and heat transfer process in soil under field conditions, especially in near surface soils [63]. Based solely on the heat pulse function of the thermo-TDR sensor, the use of a series of such sensors aligned in a soil profile permitted the determination of soil heat fluxes, liquid water fluxes, and soil-water evaporation fluxes [64].

Based on Fourier’s law, the one-dimensional heat flux density (G) can be calculated based on soil temperature gradient multiplied by soil thermal conductivity. A few studies have found that the reliability of heat flux density depends largely on the accuracy of λ determinations [65–67]. Soil temperature and λ could be measured simultaneously and in-situ with the heat pulse method. Besides, soil thermal conductivity models provided an alternative method to obtain λ . Ochsner et al. showed that the heat pulse probe worked well in obtaining λ and soil heat flux density under field conditions [66]. Peng et al. investigated λ model-based gradient methods to determine soil heat flux density [67]. Both heat pulse based and λ models based

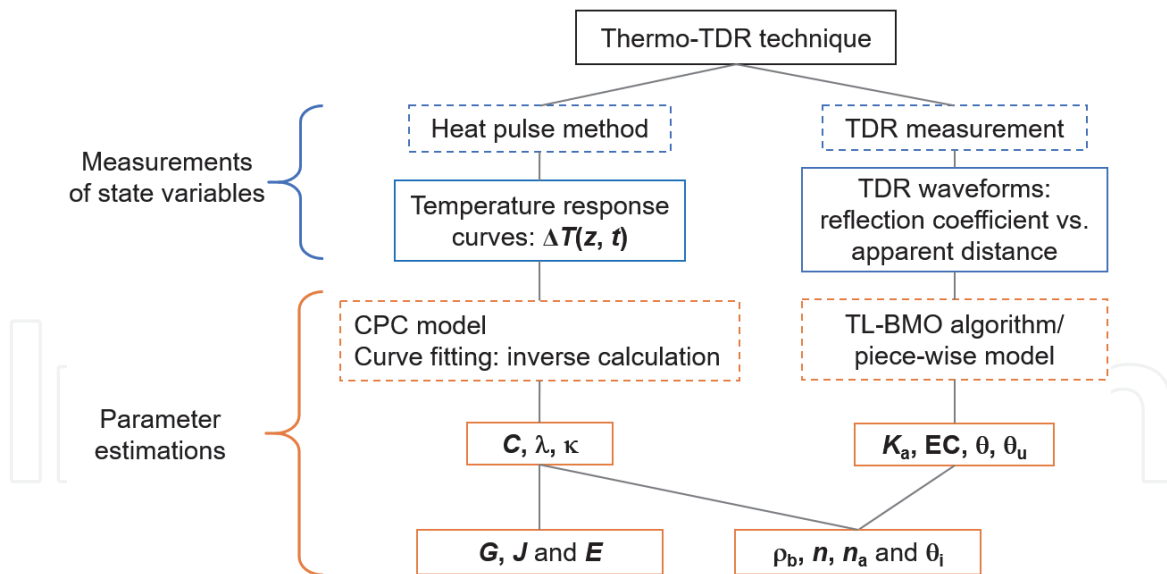


Figure 11.
The schematic view of thermo-TDR sensor measurement for state variables and parameters. (figure originally published in [22], replot in this context).

gradient methods provided reliable near-surface heat flux with continuous and variable θ , ρ_b , λ and T measurements under field conditions that included soil disturbance or deformation [66, 67].

A heat pulse technique based on the sensible heat balance of near-surface soil layers was able to determine in situ soil water evaporation (E) rates [68, 69]. The sensible heat balance method determined soil water evaporation with time and depth [70–72]. Improvements in sensor configuration enabled the determination of soil temperature, heat fluxes and storage as well as latent heat at a mm-scale [73, 74]. Heat pulse measurements of soil water evaporation dynamics also made it possible to partition evapotranspiration under field conditions [75].

An analytical solution that related soil water flux density (J) to the maximum temperature difference at upstream and downstream sensing probes was developed [76]. Then a further simplified form was established using the ratio of downstream and upstream temperatures [77]. Studies demonstrated the accuracy of the heat pulse technique to determine soil water flux [76, 78–81]. Accurate measurements of soil water flux density are necessary to quantify infiltration, runoff, solute transport, and subsurface hydraulic processes.

4. Outlook

Figure 11 presents a flowchart of the uses and outcomes for the thermo-TDR method. Generally, the thermo-TDR determined state variables and physical parameters can be estimated with proper models and methods. The most promising aspect of the thermo-TDR technique is the capability to determine in situ bulk density, porosity, heat flux, water flux and vapor flux. These provide opportunities to study transient heat and water processes in field soils, including water evaporation, sensible and latent heat, and liquid water fluxes [64, 68, 69, 82].

5. Conclusions

This chapter includes descriptions of thermo-TDR sensors, methods for collecting and analyzing data, and reviews of current and potential thermo-TDR

applications. The thermo-TDR sensor, which combines a heat pulse probe with a time domain reflectometry probe for soil thermal and electrical properties determinations, provides new opportunities for improved soil measurements on thermal properties, water content, bulk electrical conductivity, ice content, bulk density, air-filled porosity, heat flux, water flux, and vapor flux. The thermo-TDR technique has the potential to monitor in situ soil physical properties and processes for vadose zone soils.

Acknowledgements

This work was funded by the National Natural Science Foundation of China (41977011 and 41671223), the U.S. National Science Foundation (2037504) and USDA-NIFA Multi-State Project 4188.

Author details


Yili Lu^{1*}, Wei Peng¹, Tusheng Ren¹ and Robert Horton²

¹ China Agricultural University, Beijing, China

² Iowa State University, Ames IA, USA

*Address all correspondence to: luyili@cau.edu.cn

IntechOpen

© 2021 The Author(s). Licensee IntechOpen. This chapter is distributed under the terms of the Creative Commons Attribution License (<http://creativecommons.org/licenses/by/3.0>), which permits unrestricted use, distribution, and reproduction in any medium, provided the original work is properly cited. 

References

- [1] Ren, T.S., Noborio, K., & Horton, R. (1999). Measuring soil water content, electrical conductivity, and thermal properties with a thermo- time domain reflectometry probe. *Soil Science Society of America Journal*, 63, 450–457. doi:10.2136/sssaj1999.03615995006300030005x.
- [2] Lu, Y.L., Liu, X.N., Zhang, M., Heitman, J.L., Horton, R., & Ren, T.S. (2017). Thermo- time domain reflectometry method: Advances in monitoring in situ soil bulk density. *Methods Soil Analysis*, Vol. 2. doi: 10.2136/msa2015.0031
- [3] Heitman, J.L., Horton, R., Ren, T.S., & Ochsner, T.E. (2007). An improved approach for measurement of coupled heat and water transfer in soil cells. *Soil Science Society of America Journal*, 71, 872–880. doi: 10.1520/GTJ20160314.
- [4] Tian, Z.C., Heitman, J.L., Horton, R., & Ren, T.S. (2015). Determining soil ice contents during freezing and thawing with thermo-time domain reflectometry. *Vadose Zone Journal*, 14 (8).
- [5] Tian, Z.C., Ren, T.S., Kojima, Y., Lu, Y.L., Horton, R., & Heitman, J.L. (2017). An improved thermo-time domain reflectometry method for determination of ice contents in partially frozen soils. *Journal of Hydrology*, 555, 786–796.
- [6] Tian, Z.C., Lu, Y.L., Ren, T.S., Horton, R., & Heitman, J.L. (2018). Improved thermo-time domain reflectometry method for continuous in-situ determination of soil bulk density. *Soil & Tillage Research*, 178, 118–129.
- [7] Kojima Y., Nakanob, Y., Kato, C., Noborio, K., Kamiya, K., & Horton, R. (2020). A new thermo-time domain reflectometry approach to quantify soil ice content at temperatures near the freezing point. *Cold Regions Science and Technology*, 174, 103060. doi: 10.1016/j.coldregions.2020.103060.
- [8] Peng, W., Lu, Y.L., Wang, M.M., Ren, T.S., & Horton, R. (2021a). Determining water content and bulk density: The Heat Pulse method outperforms the Thermo-TDR method in high-salinity soils. *Geoderma*, in press.
- [9] Campbell, G.S., Calissendorff, K., Williams, J.H. (1991). Probe for measuring soil specific heat using a heat-pulse method. *Soil Science Society of America Journal*, 55, 291–293.
- [10] Topp, G.C., Annan, J.L., & Davis, A. P. (1980). Electromagnetic determination of soil water content: measurements in coaxial transmission lines. *Water Resources Research*, 16, 574–582.
- [11] Jones, S.B., Wraith, J.M., & Or, D. (2004). Time domain reflectometry measurement principles and applications. *Hydrological Processes*, 16, 141–153.
- [12] Noborio, K., McInnes, K.J., & Heilman, J.L. (1996). Measurements of soil water content, heat capacity, and thermal conductivity with a single TDR probe. *Soil Science*, 161, 22–28.
- [13] Ochsner, T.E., Horton, R., & Ren, T. S. (2001). Simultaneous water content, air-filled porosity, and bulk density measurements with thermo-time domain reflectometry. *Soil Science Society of America Journal*, 65, 1618–1622.
- [14] Bristow, K.L., Kluitenberg, G.J., & Horton, R. (1994). Measurement of soil thermal properties with a dual-probe heat-pulse technique. *Soil Science Society of America Journal*, 58, 1288–1294.

- [15] Kluitenberg, G.J., Ham, J.M., & Bristow, K.L. (1993). Error analysis of the heat pulse method for measuring soil volumetric heat capacity. *Soil Science Society of America Journal*, 57, 1444–1451.
- [16] Kluitenberg, G.J., Bristow, K.L., & Das, B.S. (1995). Error analysis of heat pulse method for measuring soil heat capacity, diffusivity, and conductivity. *Soil Science Society of America Journal*, 59, 719–726.
- [17] de Vries, D. A. (1952). A nonstationary method for determining thermal conductivity of soil in situ. *Soil Science*, 73(2), 83–90.
- [18] Knight, J.H., Kluitenberg, G.J., Kamai, T., & Hopmans, J.W. (2012). Semianalytical solution for dual-probe heat-pulse applications that accounts for probe radius and heat capacity. *Vadose Zone Journal*, 11(2).
- [19] Lu, Y.L., Wang, Y.J., & Ren, T.S. (2013). Using late time data improves the heat-pulse method for estimating soil thermal properties with the pulsed infinite line source theory. *Vadose Zone Journal*, 12(4).
- [20] Peng, W., Lu, Y.L., Ren, T.S., & Horton, R. (2021b). Application of infinite line source and cylindrical-perfect-conductor theories to heat pulse measurements with large sensors. *Soil Science Society of America Journal*, doi: 10.1002/saj2.20250.
- [21] Kamai, T., Kluitenberg, G.J., & Hopmans, J.W. (2015). A dual-probe heat-pulse sensor with rigid probes for improved soil water content measurement. *Soil Science Society of America Journal*, 79:1059–1072.
- [22] Peng, W., Lu, Y.L., Xie, X.T., Ren, T.S., & Horton, R. (2019). An improved thermo-TDR technique for monitoring soil thermal properties, water content, bulk density, and porosity. *Vadose Zone Journal*, 18, 190026.
- [23] Noborio, K. (2001). Measurement of soil water content and electrical conductivity by time domain reflectometry: A review. *Computers and Electronics in Agriculture*, 31, 213–237.
- [24] Wang, Z.J., Kojima, Y., Lu, S., Chen, Y., Horton, R., & Schwartz, R.C. (2014). Time domain reflectometry waveform analysis with second-order bounded mean oscillation. *Soil Science Society of America Journal*, 78, 1146–1152. doi: 10.2136/sssaj2013.11.0497.
- [25] Wang, Z.J., Lu, Y.L., Kojima, Y., Lu, S., Zhang, M., Chen, Y., & Horton, R. (2015). Tangent line/second-order bounded mean oscillation waveform analysis for short TDR probe. *Vadose Zone Journal*, 15(1). doi:10.2136/vzj2015.04.0054.
- [26] Wang, Z.J., Schwartz, R.C., Kojima, Y., Chen, Y., & Horton, R. (2017). A comparison of second-order derivative based models for time domain reflectometry waveform analysis. *Vadose Zone Journal*, 16(7). doi: 10.2136/vzj2017.01.0014.
- [27] Topp, G.C., Yanuka, M., Zebchuk, W.D., & Zegelin, S.J. (1988). The determination of electrical conductivity using TDR: soil and water experiments in coaxial lines. *Water Resources Research*, 24, 945–952.
- [28] Nadler, A., Dasberg, S., & Lapid, I. (1991). Time domain reflectometry measurements of water content and electrical conductivity of layered soil columns. *Soil Science Society of America Journal*, 55, 938–943.
- [29] Heimovaara, T.J., Focke, A.G., Bouten, W., & Verstraten, J.M. (1995). Assessing temporal variations in soil water composition with time domain reflectometry. *Soil Science Society of America Journal*, 59, 689–698.
- [30] Huisman, J.A., Lin, C.P., Weihermüller, L., & Vereecken, H.

- (2008). Accuracy of bulk electrical conductivity measurements with time domain reflectometry. *Vadose Zone Journal*, 7, 426–433.
- [31] Wang, Z.J., Timlin, D., Kojima, Y., Luo, C.Y., Chen, Y., Li, S., Fleisher, D., Tully, K., Reddy, V.R., & Horton, R. (2021). A piecewise analysis model for electrical conductivity calculation from time domain reflectometry waveforms. *Computers and Electronics Agriculture*, 182.
- [32] Blackwell, H.H. (1956). The axial-flow error in the thermal-conductivity probe. *Canadian Journal of Physics*, 34, 412–417.
- [33] Ghezzehei, T.A. (2008). Errors in determination of soil water content using time domain reflectometry caused by soil compaction around waveguides. *Water Resources Research*, 44, W08451.
- [34] Liu, X.N., Ren, T.S., & Horton, R. (2008). Determination of soil bulk density with thermo-time domain reflectometry sensors. *Soil Science Society of America Journal*, 72, 1000–1005. doi:10.2136/sssaj2007.0332.
- [35] Yu, X.B., Zhang, N., Pradhan, A., Thapa, B., & Tjuatja, S. (2015). Design and evaluation of a thermo-TDR probe for geothermal applications. *Geotechnical. Testing Journal*, 38, 864–877. doi:10.1520/GTJ20150023.
- [36] Wen, M.M., Liu, G., Horton, R., & Noborio, K. (2018). An in situ probe-spacing- correcting thermo-TDR sensor to measure soil water content accurately. *European Journal of Soil Science*, 69, 1030–1034. doi:10.1111/ejss.12718.
- [37] Olmanson, O.K., & Ochsner, T.E. (2008). A partial cylindrical thermo-time domain reflectometry sensor. *Soil Science Society of America Journal*, 72, 571–577. doi:10.2136/sssaj2007.0084.
- [38] Ren, T.S., Ju, Z.Q., Gong, Y.S., & Horton, R. (2005). Comparing heat pulse and time domain reflectometry soil water contents from thermo-time domain reflectometry probes. *Vadose Zone Journal*, 4, 1080–1086. doi:10.2136/vzj2004.0139.
- [39] Jury, W.A., & Bellantuoni, B. (1976). A background temperature correction for thermal conductivity probes. *Soil Science Society of America Journal*, 40, 608–610.
- [40] Bristow, K. L., Campbell, G. S., & Calissendorff, K. (1993). Test of a heat-pulse probe for measuring changes in soil water content. *Soil Science Society of America Journal*, 57(4), 930–934.
- [41] Liu, G., Wen, M.M., Chang, X., Horton, R., & Ren, T.S. (2013). A self-calibrated DPHP sensor for in situ calibrating the probe spacing. *Soil Science Society of America Journal*, 77, 417–421. doi:10.2136/sssaj2012.0434n.
- [42] Liu, G., Wen, M.M., Ren, T.S., Si, B. C., Horton, R., & Hu, K.L. (2016). A general in situ probe spacing correction method for dual probe heat pulse sensor. *Agricultural and Forest Meteorology*, 226, 50–56. doi.org/10.1016/j.agrformet.2016.05.011.
- [43] Zhang, M, Lu, Y.L., Ren, T.S., & Horton, R. (2020). In-situ probe spacing calibration improves the heat pulse method for measuring soil heat capacity and water content. *Soil Science Society of America Journal*, 84, 1620–1629.
- [44] Robinson, D.A., Jones, S.B., Wraith, J.M., Or, D., Friedman, S.P. (2003). A review of advances in dielectric and electrical conductivity measurement in soils using time domain reflectometry. *Vadose Zone Journal*, 2, 444–475.
- [45] de Vries, D.A. (1963). Thermal properties of soils. In: W. R. Van Wijk, editor, *Physics of plant environment*. North-Holland Publ. Co., Amsterdam. pp. 210–235.

- [46] Lu, S., Ren, T.S., Gong, Y.S., & Horton, R. (2007). An improved model for predicting soil thermal conductivity from water content. *Soil Science Society of America Journal*, 71, 8–14.
- [47] Xie, X.T., Lu, Y.L., Ren, T.S., & Horton, R. (2018). An empirical model for estimating soil thermal diffusivity from texture, bulk density, and degree of saturation. *Journal of Hydrology*, 19, 445–457.
- [48] Liu, X.N., Lu, S., Horton, R., & Ren, T.S. (2014). In situ monitoring of soil bulk density with a thermo-TDR sensor. *Soil Science Society of America Journal*, 78, 400–407. doi:10.2136/sssaj2013.07.0278.
- [49] Tian, Z.C., Lu, Y.L., Ren, T.S., Horton, R. & Heitman, J.L. (2018a). Improved thermo-time domain reflectometry method for continuous in-situ determination of soil bulk density. *Soil & Tillage Research*, 178, 118–129.
- [50] Lu, Y.L., Lu, S., Horton, R., & Ren, T. (2014). An empirical model for estimating soil thermal conductivity from texture, water content, and bulk density. *Soil Science Society of America Journal*, 78, 1859–1868.
- [51] Tian, Z.C., Horton, R., & Ren, T.S. (2016). A simplified de Vries-based model to estimate thermal conductivity of unfrozen and frozen soil. *European Journal of Soil Science*, 67, 564–572.
- [52] Ren, T.S., Ochsner, T.E., & Horton, R. (2003a). Development of thermo-time domain reflectometry for vadose zone measurements. *Vadose Zone Journal*, 2, 544–551. doi:10.2136/vzj2003.5440.
- [53] Ren, T.S., Ochsner, T.E., Horton, R., & Ju, Z.Q. (2003b). Heat-pulse method for soil water content measurement: Influence of the specific heat of the soil solids. *Soil Science Society of America Journal*, 67, 1631–1634.
- [54] Lu, Y.L., Liu, X.N., Heitman, J.L., Ren, T.S., & Horton, R. (2016). Determining soil bulk density with thermo-time domain reflectometry: A thermal conductivity based approach. *Soil Science Society of America Journal*, 80, 48–54. doi:10.2136/sssaj2015.08.0315.
- [55] Lu, Y.L., Horton, R., & Ren, T.S. (2018). Simultaneous determination of soil bulk density and water content: a heat pulse-based method. *European Journal of Soil Science*, 69, 947–952.
- [56] Fu, Y.W., Lu, Y.L., Heitman, J., & Ren, T.S. (2020). Root-induced changes in soil thermal and dielectric properties should not be ignored. *Geoderma*, 370, 114352.
- [57] Fu, Y.W., Lu, Y.L., Heitman, J., & Ren, T.S. (2020). Root influences on soil bulk density measurements with thermo-time domain reflectometry. *Geoderma*, 403, 115195.
- [58] Campbell, G. S. (1985). *Soil physics with BASIC: Transport models for soil-plant systems*, (3rd ed.). New York: Elsevier.
- [59] Zhang, N., Yu, X.B., Pradhan, A., & Puppala, A.J. (2016). A new generalized soil thermal conductivity model for sand-kaolin clay mixtures using thermo-time domain reflectometry probe test. *Acta Geotechnica*. doi: 10.1007/s11440-016-0506-0.
- [60] Zhang, N., Yu, X.B., & Pradhan, A. (2017a). Application of a thermo-time domain reflectometry probe in sand-kaolin clay mixtures. *Engineering Geology*, 216, 98–107. doi: 10.1016/j.enggeo.2016.11.016.
- [61] Zhang, N., Yu, X.B., & Wang, X.L. (2017b). Use of a thermo-TDR probe to measure sand thermal conductivity dryout curves (TCDCs) and model prediction. *International Journal of Heat and Mass Transfer*, 115, 1054–1064.

- [62] Zhang, N., Yu, X.B., & Wang, X.L. (2018). Validation of a thermo-time domain reflectometry probe for sand thermal conductivity measurement in drainage and drying processes. *Geotechnical Testing Journal*, 41, 403–412. doi: 10.1520/GTJ20160314.
- [63] He, H.L., Dyck, M.F., Horton, R., Ren, T.S., Bristow, K.L., Lv, J., & Si, B. C. (2018). Development and application of the heat pulse method for soil physical measurements. *Reviews of Geophysics*, 56, 567–620.
- [64] Heitman, J.L., Zhang, X., Xiao, X., Ren, T.S., & Horton, R. (2017). Advances in heat-pulse methods: measuring soil water evaporation with sensible heat balance. In: Logsdon, S. (Ed.), *Methods of Soil Analysis. Soil Science Society of America*, Madison, WI, Vol. 2 (1).
- [65] Evett, S. R., Agam, N., Kustas, W. P., Colaizzi, P. D., & Schwartz, R. C. (2012). Soil profile method for soil thermal diffusivity, conductivity and heat flux: Comparison to soil heat flux plates. *Advances in Water Resources*, 50, 41–54.
- [66] Ochsner, T. E., Sauer, T. J., & Horton, R. (2006). Field tests of the soil heat flux plate method and some alternatives. *Agronomy Journal*, 98, 1005–1014.
- [67] Peng, X.Y., Wang, Y.Y., Heitman, J. L., Ochsner, T., Horton, R., & Ren, T.S. (2017). Measurement of soil-surface heat flux with a multi-needle heat-pulse probe. *European Journal of Soil Science*, 68, 336–344.
- [68] Heitman, J.L., Horton, R., Sauer, T. J., & Desutter, T.M. (2008a). Sensible heat observations reveal soil-water evaporation dynamics. *Journal of Hydrology*, 9, 165–171. doi:10.1175/2007JHM963.1
- [69] Heitman, J.L., Xiao, X., Horton, R., & Sauer, T.J. (2008b). Sensible heat measurements indicating depth and magnitude of subsurface soil water evaporation. *Water Resources Research*, 44, W00D05.
- [70] Sakai, M., Jones, S.B., & Tuller, M., (2011). Numerical evaluation of subsurface soil water evaporation derived from sensible heat balance. *Water Resources Research*, 47 (2).
- [71] Xiao, X., Horton, R., Sauer, T.J., Heitman, J.L., & Ren, T.S. (2011). Cumulative soil water evaporation as a function of depth and time. *Vadose Zone J.* 10, 1016–1022. doi:10.2136/vzj2010.0070
- [72] Deol, P., Heitman, J.L., Amoozegar, A., Ren, T.S. & Horton, R. (2012). Quantifying nonisothermal subsurface soil water evaporation. *Water Resources Research*, 48, W11503.
- [73] Zhang, X., Lu, S., Heitman, J.L., Horton, R., & Ren, T.S., (2012). Measuring subsurface soil-water evaporation with an improved heat-pulse probe. *Soil Science Society of America Journal*, 76, 876–879. doi: 10.2136/sssaj2011.0052n
- [74] Xiao, X., Zhang, X., Ren, T.S., Horton, R., & Heitman, J.L. (2015). Thermal property measurement errors with heat-pulse sensors positioned near a soil-air interface. *Soil Science Society of America Journal*, 79, 766–771.
- [75] Wang, Y. Y., Horton, R., Xue, X. Z., & Ren, T.S. (2021). Partitioning evapotranspiration by measuring soil water evaporation with heat-pulse sensors and plant transpiration with sap flow gauges. *Agricultural Water Management*, 252, 106883.
- [76] Ren, T.S., Kluitenberg, G.J., & Horton, R. (2000). Determining soil water flux and pore water velocity by a heat pulse technique. *Soil Science Society of America Journal*, 64, 552–560.
- [77] Wang, Q., Ochsner, T.E., & Horton, R. (2002). Mathematical analysis of heat

pulse signals for soil water flux determination. *Water Resources Research*, 38, doi:10. 1029/2001WR1089.

[78] Mori, Y., Hopmans, J.W., Mortensen, A.P., & Kluitenberg, G.J. (2003). Multi-functional heat pulse probe for the simultaneous measurement of soil water content, solute concentration, and heat transport parameters. *Vadose Zone Journal*, 2, 561–571.

[79] Mori, Y., Hopmans, J.W., Mortensen, A.P., & Kluitenberg, G.J. (2005). Estimation of vadose zone water flux from multi-functional heat pulse probe measurements. *Soil Sci. Soc. Am. J.* 69, 599–606.

[80] Ochsner, T.E., Horton, R., Kluitenberg, G.J., & Wang, Q. (2005). Evaluation of the heat pulse ratio method for measuring soil water flux. *Soil Science Society of America Journal*, 69, 599–606.

[81] Gao, J.Y., Ren, T.S., & Gong, Y.S. (2006). Correcting wall flow effect improves the heat-pulse technique for determining water flux in saturated soils. *Soil Science Society of America Journal*, 70, 711–717.

[82] Tian, Z.C., Kool, D., Ren, T.S., Horton, R., & Heitman, J.L. (2018b). Determining in-situ unsaturated soil hydraulic conductivity at a fine depth scale with heat pulse and water potential sensors. *Journal of Hydrology*, 564, 802–810.